LIMNOLOGY and OCEANOGRAPHY

ASLO

Limnol. Oceanogr. 69, 2024, 2624–2638

doi: 10.1002/lno.12690

Strong large-scale structure–function coupling in benthic bacteria is mediated by algae in a geodiverse river network

Lukas Thuile Bistarelli [1,2] **Thomas Fuß** [1,2] **Franziska Walther** [3] **Luca Zoccarato** [1,4,5] **Lauren Talluto** [2] **Anna M. Romaní** [6] **Hans-Peter Grossart** [1,7] **Gabriel A. Singer** [1,2*]

[1]Leibniz-Institute of Freshwater Ecology and Inland Fisheries (IGB), Berlin, Germany
[2]Institute of Ecology, University of Innsbruck, Innsbruck, Austria
[3]Planning of Landscape and Urban Systems, Institute for Spatial and Landscape Development, ETH Zürich, Zürich, Switzerland
[4]Core Facility Bioinformatics, University of Natural Resources and Life Sciences, Vienna, Vienna, Austria
[5]Department of Biotechnology, Institute of Computational Biology, University of Natural Resources and Life Sciences, Vienna, Vienna, Austria
[6]Institute of Aquatic Ecology, University of Girona, Girona, Spain
[7]Institute of Biochemistry and Biology, Potsdam University, Potsdam, Germany

Abstract

Benthic bacteria in stream ecosystems drive organic matter mineralization. However, knowledge on how this ecosystem function is driven by bacterial community composition in interaction with environmental conditions and organic matter resources is poor. This is especially true when considering the regional scale of river networks, at which environmental conditions vary in a scale-dependent manner and are spatially structured due to asymmetrical water flow. Similarly, organic matter resources may have a terrestrial origin in remote headwaters or be sourced locally from algae living in close proximity to bacteria in benthic biofilms. We investigated benthic biofilm meta-community structure and function across the > 6700 km^2 river network of the near-natural Vjosa in Albania and Greece and found a strong control of the benthic algal community on bacterial community composition (13.4% of variability explained). In addition, bacterial community composition has linkages to water chemistry, which itself is strongly shaped by the diverse geology in the catchment, and to dispersal, shaping metacommunity structure as a neutral process. Notably, bacterial community composition explained the largest single fraction of variability (31.5%) in extracellular enzymatic activities, while there was no dependency of enzyme ratios on organic matter nor environmental conditions. Synergistic effects between bacteria and algae accounted for additional 47.3% of variability in heterotrophic functioning, emphasizing the importance of algal–bacterial interactions in benthic biofilms. Our findings shed new light on bacterial structure–function coupling highlighting the importance of algal–bacterial interactions at the river network scale.

In fluvial ecosystems, organic matter breakdown, a major aspect of ecosystem functioning, is strongly tied to benthic biofilms (Romaní et al. 2004; Battin et al. 2016; Fabian et al. 2018), where heterotroph bacteria secrete extracellular enzymes to break down dissolved organic matter (DOM) (Romaní et al. 2012). Despite intensive research on natural biofilms in rivers in recent years, heterotrophic biofilm functioning remains poorly understood due to the high bacterial biodiversity, the chemical complexity of natural DOM, and the various processes shaping both of these controls across multiple spatial scales. Additionally, biological interactions between bacteria, algae, and fungi within the biofilm can alter the bacterial community composition (Zancarini et al. 2017; Fell et al. 2021) and therefore indirectly affect heterotrophic functioning. Conceptually, bacterial community composition

*Correspondence: gabriel.singer@uibk.ac.at

Additional Supporting Information may be found in the online version of this article.

Author Contribution Statement: LTB and GAS designed the research. LTB, GAS, TF, LT, and FW organized the field campaign and contributed to sampling. LTB and TF performed biofilm sampling and community analysis. LTB performed enzyme incubations in the field and measurements in the lab. AMR and LTB designed the enzyme assay. LTB performed statistical analysis with the support of TF, FW, LT, AMR, LZ, and GAS. LTB wrote the first draft of the manuscript and all authors gave feedback and contributed significantly to revisions.

(Freimann et al. 2013) and biodiversity (Cardinale et al. 2002; Delgado-Baquerizo et al. 2016) are recognized as important factors influencing functioning in freshwater ecosystems. And, indeed, the high chemical diversity of freshwater DOM (Mosher et al. 2015) may require high bacterial biodiversity to fully exploit the available chemical diversity and thereby maintain DOM breakdown. However, the rules governing distribution of DOM at various spatial scales are different from those driving benthic microbial community differentiation, and as traits of available resources need to match with the functional capabilities of the consumers, higher bacterial diversity alone does not necessarily translate into increased functioning by complementary resource use (Talluto et al. 2024).

At the microhabitat scale, several studies found that flow velocity (Battin et al. 2003; Niederdorfer et al. 2016) and biomass (Battin et al. 2016) affect benthic biofilm microarchitecture with consequences for biofilm functioning (Singer et al. 2011). The close proximity of different organisms in the biofilm matrix is thought to benefit functioning through complementarity (Costerton et al. 1995; Loreau et al. 2001; Battin et al. 2016). Prominent examples for proximity-enhanced interactions are labile algal exudates, that is, autochthonous DOM, which can be easily metabolized by the bacterial community (Pérez and Sommaruga 2006; Ramanan et al. 2016; Wagner et al. 2017). These interactions however do not only benefit bacteria. The provision of microhabitat structure can go both ways and while bacteria rely on DOM from algae, they provide mineralization-derived inorganic carbon as well as micronutrients and macronutrients to the algal community (Kouzuma and Watanabe 2015; Ramanan et al. 2016; Wagner et al. 2017). Through these interactions algal communities, especially in phototrophic biofilms, may play an important role in structuring benthic bacterial communities and driving biofilm functioning (Zancarini et al. 2017; Fabian et al. 2018). In concordance with this notion, it was shown that alterations in light availability induce changes in benthic bacterial community composition and functioning (Wagner et al. 2017; Seballos et al. 2020). Lastly, algal–bacterial interactions can also be negative, such as in the case of competition for nutrients or algal cell lysis by bacteria (Ramanan et al. 2016).

At the scale of river networks, the exchange of resources, energy, and organisms among local habitats in a river network is important. Local bacterial communities are connected to a regional metacommunity by dispersal, and terrestrially derived DOM from headwaters can fuel heterotrophic metabolism at far downstream sites. Such processes that connect local habitats throughout the entire river network have led to the recognition of river networks as fluvial meta-ecosystems (Loreau et al. 2003). A key property of fluvial meta-ecosystems is their hierarchical and dendritic structure (Benda et al. 2004), which together with the asymmetrical nature of fluvial meta-ecosystems imposed by the unidirectional flow of water restricts transport of energy, resources, and bacterial dispersal. The terrestrial matrix influences the physicochemical environment (Fuß et al. 2017) and structures bacterial communities through inoculation from soils (Crump et al. 2012). A recent study by Fuß et al. (2024) confirms that catchment geology exerted the strongest control on water chemistry and temperature across the Vjosa River network. In turn, water chemistry is suggested as a major driver of bacterial community composition and diversity mainly through conductivity and pH (Freimann et al. 2013). Besides deterministic controls on benthic bacteria, regionally acting spatial processes related to dispersal, extinction, and colonization also play a role at the level of the metacommunity that is hosted by the entire river network. In fact, metacommunity theory provides useful paradigms to better understand scale-dependent mechanisms behind community composition and diversity in fluvial meta-ecosystems (Leibold et al. 2004): Species sorting emphasizes the local selection of species through environmental variables and seems to be the dominant paradigm governing community assembly in fluvial networks (Heino et al. 2015). Some dispersal is needed for efficient sorting (Van der Gucht et al. 2007), but higher dispersal may also drive mass effects, which allow continued survival of badly adapted species in seemingly suboptimal habitats (Leibold et al. 2004). However, the strength with which these paradigms affect bacterial communities is linked to their lifestyle. Benthic bacteria show stronger effects of species sorting and free-living bacteria are more prone to mass effects (Gweon et al. 2021; Wisnoski and Lennon 2021).

Chemically diverse DOM can shape bacterial communities and drive heterotroph functioning. In fluvial networks, DOM shows distinct spatial patterns (Creed et al. 2015; Mosher et al. 2015) that would support a "sorting" role of this resource at river network scale. Indeed, headwaters are intimately linked to their surrounding environment and show a high differentiation in DOM composition and concentration with a strong imprint of terrigenous DOM (Creed et al. 2015; Mosher et al. 2015). With downstream movement, increasing in-stream carbon production, such as labile algal exudates, enriches the DOM sourced from upstream ecosystems (Creed et al. 2015). Thus, downstream homogenization of dissolved organic carbon concentration and predictable shifts in DOM composition occur (Mosher et al. 2015). However, these spatial resource gradients are dependent on flow dynamics, for example, terrigenous DOM may be "shunted" far downstream during times of higher discharge (Raymond et al. 2016). Also, the fact that within biofilms, autochthonous DOM may be made available to heterotrophs in immediate vicinity of its production by autotrophs further indicates the potential of DOM being a locally acting sorting factor (Wagner et al. 2017; Fabian et al. 2018). Hence, DOM can be considered a dynamic resource acting as a sorting agent and challenging the bacterial communities to efficient resource use implying a match of resource and functional traits.

To better understand in-stream carbon cycling, there is a need to study regional processes that shape patterns of bacterial community composition, DOM, and functioning simultaneously (Talluto et al. 2024). There is evidence for functional

gradients in river networks: for instance, Freixa et al. (2016) found a transition from allochthonous to autochthonous DOM utilization by the bacterial communities from upstream to downstream. However, we still lack a comprehensive understanding on how functioning unfolds at large spatial scales and the mechanisms controlling it. For instance, whether benthic bacterial community composition controls network-wide functioning patterns is still strongly debated. Some studies suggest that bacterial communities affect functioning (Findlay and Sinsabaugh 2006), while others highlight that the strength of this linkage may depend on environmental factors (Freimann et al. 2013; Battin et al. 2016). In this context, functional redundancy, that is, multiple species carrying the same set of functions (Louca et al. 2018), may play a crucial role (Freimann et al. 2013). This mechanism shifts the focus away from the taxonomic composition of bacterial communities and towards the pool of functions that these communities hold. Several studies report on functional redundancy in bacterial communities (Freixa et al. 2016; Louca et al. 2018), while others reveal that distinct bacterial communities in aquatic systems lead to distinct functional capacities (Delgado-Baquerizo et al. 2016). In summary, it is still debatable to what extent community composition reflects the functional capacity of a community. Notably, the set of functions investigated (bulk functions like growth or primary/secondary production vs. specific functions like production of specific enzymes) will strongly affect whether functional redundancy can be detected.

Here, we investigate controls on structure–function coupling in benthic bacterial communities at the scale of an entire river network. We hypothesize that bacterial community composition is controlled by (i) the algal community composition, as a proxy for local biofilm control (i.e., by the algal–bacterial interactions such as bacterial feeding on algal released DOM or the bacterial use of microhabitat structures provided by algal development); (ii) water chemistry as a main environmental filter; (iii) spatial features of the river network that govern dispersal processes; and (iv) terrigenous DOM acting as a resource filter (Fig. 1a). In turn, heterotrophic benthic biofilm functions, measured through various extracellular enzymes involved in DOM breakdown, are hypothesized to be driven by (i) bacterial community composition and (ii) available resources. The latter again can be described by terrigenous DOM and algal community composition. The dual role of resources is explored by their simultaneous consideration as resource filters acting on the bacterial communities as well as directly interacting with the bacterial communities to drive functioning (Fig. 1a).

Methods

Study area and sampling

We sampled 46 sites covering the entire river network of the Vjosa River in northern Greece and southern Albania (Fig. 1b). The Vjosa is the second largest river in Albania with a total length of 272 km and a catchment area of 6706 km^2. From a hydromorphological perspective, the Vjosa is one of the most natural river systems on the European continent (Schiemer et al. 2020). The sampling campaign took place during a 3-week period in April/May 2018. We focused the empirical work on confluences by sampling each tributary 50–150 m upstream of the confluence, and the mainstem downstream of the confluence where complete mixing across the river was detectable by measuring conductivity along transects. As there are fewer tributaries entering in the Vjosa downstream, we sampled at additional sites along the mainstem of the river.

To sample epilithic biofilms, we collected 9–13 stones at each site in a way that pool and riffle sequences were equally represented. Biofilm from the sun-facing side of stones was removed using previously flamed scalpels and put into sterile 50-mL Falcon tubes. The slurry was homogenized using a flamed frother and subsamples of 1 mL were taken for characterization of bacterial communities. Following addition of 1 mL of 99% ethanol, these samples were stored in a portable freezer. A frozen slurry was also kept for further analysis of chlorophyll *a* (Chl *a*). Potential extracellular enzyme activity was assessed using a deep-well plate design (*see* below) and inoculated with subsamples from the homogenized and fresh biofilm slurry. Streamwater samples were collected using a 60-mL syringe and subsequently filtered through 0.2-μm membrane filters (Sartorius, Germany) to determine dissolved organic carbon concentrations, DOM characteristics, and a suite of water chemical variables. Conductivity, pH, and temperature were measured on-site using a WTW probe (Xylem, Germany).

Spatial structure of the river network

We generated the digital river network and delineated catchment areas for each sampling site based on a 25-m resolution digital elevation model from the European Union's Earth Observation Program Copernicus. Dissolved organic matter sourced from the terrestrial environment or produced in-stream as well as bacterial cells are propagated through the river network mainly by passive downstream transport. To unravel these directional spatial processes, we performed an asymmetric eigenvector maps analysis (Blanchet et al. 2008a) based on flow-connected sites. To compute spatial variables, which describe the spatial structure of the river network, we performed a principal component analysis on a site-by-edge matrix for all 46 sites. The site-by-edge matrix is an unweighted binary matrix, which captures flow direction and the connections of sites in the whole river network. We weighted this matrix using water travel time (tt, computed based on a discharge–velocity power model) by using a decay function for each edge between flow connected sites: weights = $1 - (\mathrm{tt}/\mathrm{ttmax})^{0.5}$ (Dray et al. 2006; Fuß et al. 2024). The weights represent discharge-corrected time for transport of water from an upstream to the next downstream site. To compute the weighted site-by-edge matrix we computed the Hadamard product among the site-by-edge matrix and the weights. To identify spatial variables that describe only

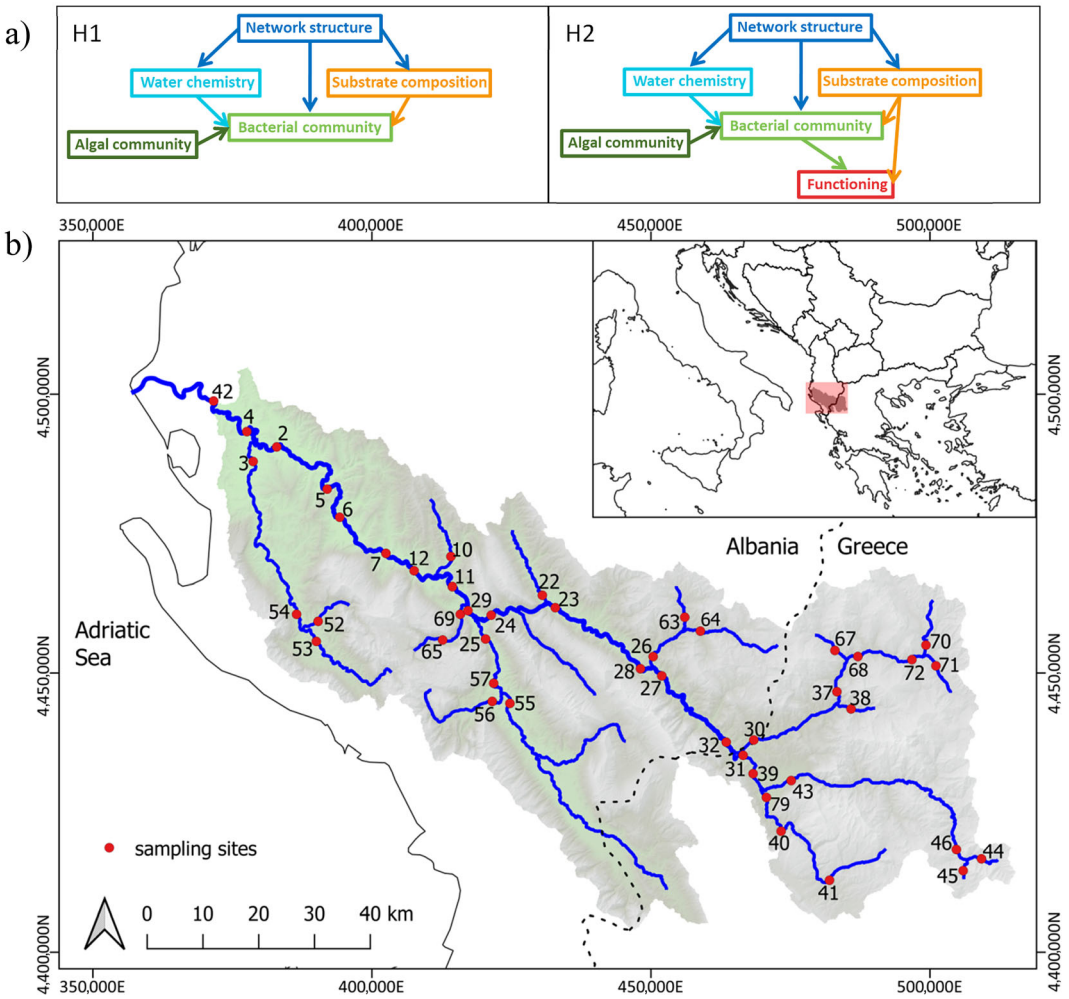

Fig. 1. (**a**) Conceptual figure detailing our hypotheses. H1 shows variables controlling bacterial communities throughout the Vjosa while H2 adds controls of heterotrophic functioning of benthic in-stream biofilms. (**b**) Map of the Vjosa River network in Albania and Greece including all sampling sites represented as red dots.

downstream processes we computed Moran's *I* and selected 15 spatial variables as they showed a significantly positive spatial autocorrelation (Blanchet et al. 2008a). The whole analysis was performed in R version 3.5 (R-Development-Core-Team 2014) using the packages aem (Blanchet et al. 2015) and WatershedTools (Talluto 2019).

Water chemistry and geodiversity across the entire river network

We analyzed water samples for the elements Ca^{2+}, K^{+}, Mg^{2+}, S^{2-}, Si^{4+}, and Na^{+} using an ICP-OES Thermo iCAP 6000 optical emission spectrometry device (Thermo Scientific Fisher). Samples for the elements SO_4^{2-}, Cl^{-}, NO_3^{-}, and PO_4^{3-} were filtered into Eppendorf tubes and analyzed using a Dionex ICS-2000 ion chromatography device (Thermo Scientific Fisher). We found that soluble reactive phosphorus concentrations were below detection limit ($< 0.01\ mg\ L^{-1}$) at all sites and therefore excluded it from further analysis. As a major determinant for river network-wide water chemistry, we explored geological conditions in the entire Vjosa River catchment (Supporting Information Fig. S1). To this aim, geological spatial data for Albania (Institute of Geological Research and the Oil and Gas Institute of Albania 2002) and Greece (European Geological Data Infrastructure 2018) were combined and crossed with the delineated catchments for each sampling site (*see* Supporting Information S1) in the geographical information system QuantumGIS 2.18 (Quantum GIS Development Team 2015).

Concentration and optical properties of dissolved organic matter

Water samples collected at each site were filtered through a 0.2-μm membrane filter (Sartorius) into acid washed and precombusted (450°C for 3 h) 20-mL glass vials with teflon-coated silicon septa, stored in a portable fridge at 4°C on site, and analyzed in the laboratory. Dissolved organic carbon

concentrations were analyzed by high temperature combustion on a multi N/C 2100 s (Analytik Jena). We measured absorbance spectra and fluorescence excitation–emission matrices using an Aqualog (Horiba Ltd) with a 1-cm quartz cuvette and used MilliQ as a blank. Absorbance spectra were measured from 250 to 600 nm with an increment of 5 nm. Excitation–emission matrices were excited from 250 to 450 nm with an increment of 5 nm and emissions were measured from 250 to 600 nm with an increment of 3.2 nm.

We computed (i) the specific UV absorption at 254 nm ($SUVA_{254}$) divided by the dissolved organic carbon concentration, which correlates strongly with aromaticity (Weishaar et al. 2003); (ii) $E2 : E3$ as the absorbance ratio at 250 : 365 nm as an indicator for molecular weight; and (iii) $E4 : E6$ as the absorbance ratio at 465 : 600 nm, which correlates to the degree of humification. We also computed Naperian absorption coefficients and used them to compute the slope ratio according to Helms et al. (2008), which correlates inversely with molecular weight. Excitation–emission matrices were corrected for Raman scattering by subtracting the blank from the sample, Rayleigh scattering was removed by the Aqualog software directly and 2nd-order Rayleigh scattering was set to zero (McKnight et al. 2001). We used corrected excitation–emission matrices to compute (i) total fluorescence; (ii) fluorescence index, which provides information whether the DOM is of terrestrial or microbial origin (McKnight et al. 2001); (iii) humification index, which indicates the degree of humification (Zsolnay et al. 1999); and (iv) beta/alpha, which represents freshness of DOM (Zsolnay et al. 1999).

DNA extraction and sequencing

DNA extraction was performed following the protocol of Nercessian et al. (2005) with slight modifications (*see* Supporting Information S2). Cleaned DNA was dissolved in 50 μL PCR-grade water and frozen at −20°C for further analysis. DNA concentrations were assessed using a Quantus Fluorometer (Promega). DNA extracts were submitted to LGC Genomics (Berlin, Germany) for PCR using the primers 341F 5′-CCTACGGGGG CWGCAG-3′ and 785R 5′-GACTACHVGGGTATCTAAKCC-3′ (Klindworth et al. 2013), sequencing on an Illumina MiSeq platform using a 300-base-pair paired-end sequencing, and initial bioinformatics (i.e., demultiplexing, adapter and primer clipping). Primer-clipped sequences were denoised following the DADA2 workflow with default settings (Callahan et al. 2016) yielding 2404 amplicon sequence variants (ASVs) at 42 sites.

Functions: Measurements of extracellular enzyme activities

We measured the potential activity of eight extracellular enzymes: β-glucosidase (Glu, EC 3.2.1.21) and cellobiohydrolase (Cbh, EC 3.2.1.91) are involved in cellulose degradation; β-xylosidase (Xyl, EC 3.2.1.37) is involved in hemicellulose degradation; leucine aminopeptidase (Pep, EC 3.4.11.1) decomposes peptides; phenol oxidase (Pox, EC 1.14.18.1) degrades lignin; lipase (Lip, EC 3.1.1.3) decomposes lipids; β-*N*-acetylglucosaminidase (NAG, EC 3.2.1.52) is involved in chitin decomposition; and phosphatase (Pho, EC 3.1.3.1–2) is involved in phosphorus acquisition. Leucine aminopeptidase activity was measured using a 7-amino-4-methylcoumarin hydrochloride-linked artificial substrate, phenol oxidase was measured using L-3,4-dihydroxyphenylalanine, and all other enzyme activities were assessed using artificial substrates linked to methylumbelliferone. All enzyme assays were done in a priori prepared 96-well deep plates incubated on-site under water in a dark waterproof container for 1 h. Thereafter, incubations were stopped using buffers and freezing of the plates in the field. In the laboratory, deep-well plates were thawed, gently centrifuged to remove sediment particles and 200 μL of supernatant were transferred into black 96-well plates with clear bottom (Greiner Bio-One) to measure fluorescence and absorbance with a plate reader (Tecan Trading AG). Enzyme activity data were used to compute enzyme ratios as biomass-independent measures of heterotrophic biofilm functioning (Supporting Information Table S1). See Supporting Information S3 for more details.

Algal community composition and biomass

In a parallel study carried out in the same time period, Fuß et al. (2024) investigated the controls of metacommunity structure and function of periphytic algae. The sampling protocol for the algal community was identical to our sampling, with the only difference that instead of bacterial primers, diatom-specific primers were used for the amplicon sequencing. As part of their analysis, they performed a principal component analysis on the site-by-species table of algae, which we used as an explanatory matrix for bacterial community composition. Frozen Chl *a* samples were extracted with dimethylformamide and analyzed on a high-performance liquid chromatography (Fuß et al. 2024). We measured the area of the scraped stones with image analysis of high-angle photographs and used the area to correct the Chl *a* values, which served as a proxy for algal biomass.

Data analyses

Bacterial community composition and diversity

To improve comparability, samples with small library sizes (< 1000 reads per sample) were excluded from the analysis and the remaining samples ($n = 28$) were rarified to the lowest number of reads per sample (3435) to account for different sequencing efforts. For further analysis, we excluded ASVs that had a raw read count of < 5 per site to reduce the chance for spurious relationships in downstream data analysis (Blanchet et al. 2014). Thereafter, the site-by-ASV table was Hellinger-transformed and translated into a Bray–Curtis dissimilarity matrix. The dissimilarity matrix was used to compute a non-metric multidimensional scaling to visualize metacommunity structure. To better elucidate metacommunity patterns, dots in the nmds plot were grouped according to three catchment area size classes: headwaters < 350 km^2; mid-reaches ≥ 350 km^2 and < 3000 km^2; low-reaches ≥ 3000. To be able to use bacterial

community composition as a constraint in the variation partitioning step with enzyme ratios as responses (*see* "Partitioning metacommunity structure–functioning" section), we performed a principal component analysis on the Hellinger transformed site-by-ASV table as a dimensionality reduction technique. From the site-by-ASV table, we computed Shannon Diversity using R version 3.5 and the package vegan (Oksanen et al. 2019). We applied general additive models for location, scale, and shape using the R package gamlss (Rigby and Stasinopoulos 2005) to analyze trends in mean and variability of Shannon diversity.

Co-occurrence network analysis

To assess whether global bacterial network properties change from upstream to downstream, we inferred sparCC co-occurrence networks (Friedman and Alm 2012) using the sparcc function from the R package SpiecEasi (Kurtz et al. 2015). We split the site-by-ASV table in three, following the catchment area size classes used for the nonmetric multidimensional scaling (< 350, ≥ 350 and < 3000, and ≥ 3000 km^2). The site-by-ASV tables were transformed using robust center-log-ratio, as this accounts for sparse and compositional data (Friedman and Alm 2012), before computing the sparCC correlations. Correlations were retained if their absolute value was > 0.3. We clustered subnetworks by applying a hierarchical agglomeration algorithm which optimizes subnetwork modularity (Clauset et al. 2004) using the fastgreedy.community function from the R package igraph (Csardi and Nepusz 2006) and computed modularity and average path length using the functions modularity and average.path.length from the R package igraph. Modularity represents the degree of compartmentalization of a network (Faust and Raes 2012), and average path length is linked to a network's response time to perturbations (Faust and Raes 2012).

Partitioning metacommunity structure–function

To assess explained variation of bacterial community composition and enzyme ratios, we performed variation partitioning using redundancy analysis with multiple predictor matrices. For this, we first regressed bacterial community composition as a response matrix on one of four predictor matrices in separate redundancy analyses: (i) principal components of the algal community composition (*see* Fuß et al. 2024) and Chl *a* as a proxy for algal biomass, (ii) water chemistry variables, (iii) selected spatial variables, and (iv) DOM variables. Similarly, we used enzyme ratios as response matrix in separate redundancy analyses with one of four predictor matrices: principal components of bacterial and algal communities, DOM variables, and spatial variables. Significant redundancy analysis models were followed by a forward selection based on adjusted R^2 and p-value (Blanchet et al. 2008a,b, 2011). The selected variables were then used to define updated predictor matrices in the two final variation partitioning analyses. For example, with enzyme ratios as response, variation was partitioned into components purely attributable to bacterial and algal communities (redundancy analysis models for DOM and spatial variables were not significant) and to a fraction shared by both bacteria and algae. In the case of algal principal components as predictors for bacterial communities and bacterial principal components as predictors for enzyme ratios, we retained principal components that individually explained at least 3% of the variability of the respective data to ensure an appropriate type 1 error for the global redundancy analysis models, which constitute the basis of predictor selection (Blanchet et al. 2008a). All analyses were performed using R 3.5. For principal component analysis, redundancy analysis, and variation partitioning we used the package vegan (Oksanen et al. 2019), for the forward selection we used the package packfor (Dray et al. 2016).

Results

Spatial patterns of bacterial diversity and metacommunity structure

After data processing, we retained 1132 ASVs at 28 sites. Local ASV diversity ranged from 3.98 to 5.25. Nonmetric multidimensional scaling based on Bray–Curtis dissimilarity showed a beta-diversity decrease with increasing stream size (Fig. 2a). In agreement with this downstream compositional homogenization, we further found that variation in Shannon diversity significantly decreased with catchment area, while mean Shannon diversity increased with increasing stream size, albeit not significantly (Fig. 2b). Co-occurrence networks for the three catchment area size classes reflecting headwaters, mid- and low-reaches showed a decrease of modularity and average path length from upstream to downstream (Fig. 3).

Algal community, water chemistry, and spatial variables structure bacterial communities

Redundancy analysis followed by variation partitioning revealed that the most important explanatory matrix was the algal community accounting for 13.4% of the variation in bacterial communities with algal principal components 1, 2, 3, 4, 5, 7, and 8 selected (Fig. 4a). Among the water chemistry variables NO_3^-, K^+, Si^{4+}, SO_4^{2-}, and conductivity were selected and explained 8.2% of the variation in bacterial communities. Spatial variables 1, 2, 4, 11, 13, and 15 were selected and accounted for 6.9% of the variation. For DOM, only $SUVA_{254}$ was selected and explained 0.2% of the variation in bacterial communities. Algal community composition and spatial variables together explained another 8.3%, while algal community composition together with water chemistry accounted for 5% of the variation. Lastly, algal community composition, water chemistry, and spatial variables together accounted for 4.3% of the variation in bacterial community composition.

The algal community was used in this study with the sole purpose of explaining variation in the bacterial community composition. For an in-depth understanding of the algal community structure across the Vjosa River network, see Fuß et al. (2024). All algal principal components except principal

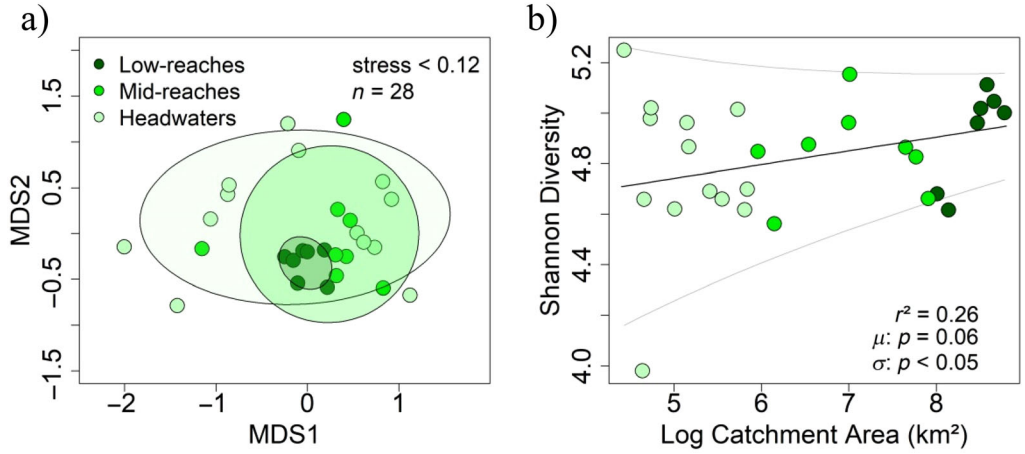

Fig. 2. (**a**) Nonmetric multidimensional scaling of bacterial community composition for three different size classes: headwaters < 350 km^2; mid-reaches ≥ 350 km^2 and < 3000 km^2; low-reaches ≥ 3000 km^2. Ellipses represent 75% confidence intervals. (**b**) General additive models (GAMLSS) of Shannon diversity vs. the logarithm of catchment area with mean (μ) and variance (σ) estimates. $n = 28$.

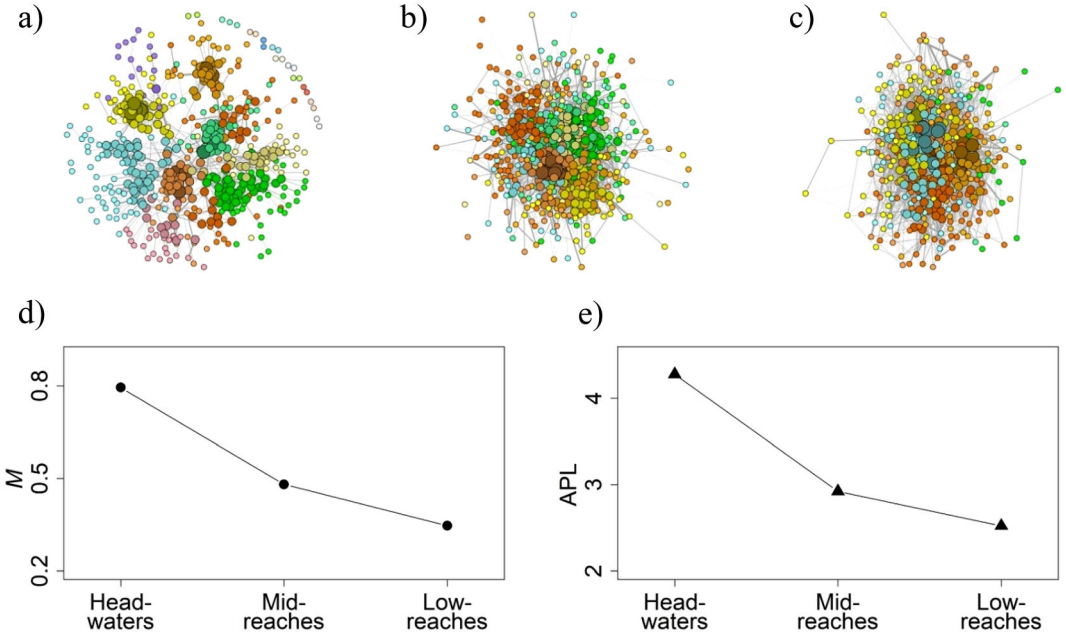

Fig. 3. (**a**–**c**) Co-occurrence networks computed using the sparCC method for sites in the headwaters, mid- and low-reaches, respectively. Node size reflects connectivity within the network while edge size reflects correlation strength. Colors show clusters with color darkness indicating a gradient from low to high connectivity. (**d**) Shows the modularity (*M*) and (**e**) the average path length (APL) of the networks.

component 6 were selected as important variables controlling bacterial communities. Chlorophyll *a*, as a proxy for algal biomass, was not selected in the variation partitioning as relevant for bacteria, but we found that with increasing stream size, Chl *a* values increased (Supporting Information Fig. S2).

Asymmetric eigenvector map analysis identified 15 spatial variables, which revealed potential spatial patterns or processes in the river network from small to regional scales. As the primary purpose of the spatial variables was to unravel what spatial structures influence bacterial communities, we focused here on those that were identified as important in the redundancy analysis with bacterial community composition as response matrix. Spatial variable 1 described a gradient from upstream to downstream and correlated strongly with subcatchment area (linear regression, $R^2 = 0.99$, df = 44, p-value < 0.001; Supporting Information Fig. S3). Spatial variable 2 differentiated sites at a main tributary of the Vjosa, the Drinos, and sites on the Vjosa mainstem upstream of the confluence. Spatial variable 4 differentiated between sites situated in the Sarantaporos and the Aoos catchments, and spatial variable

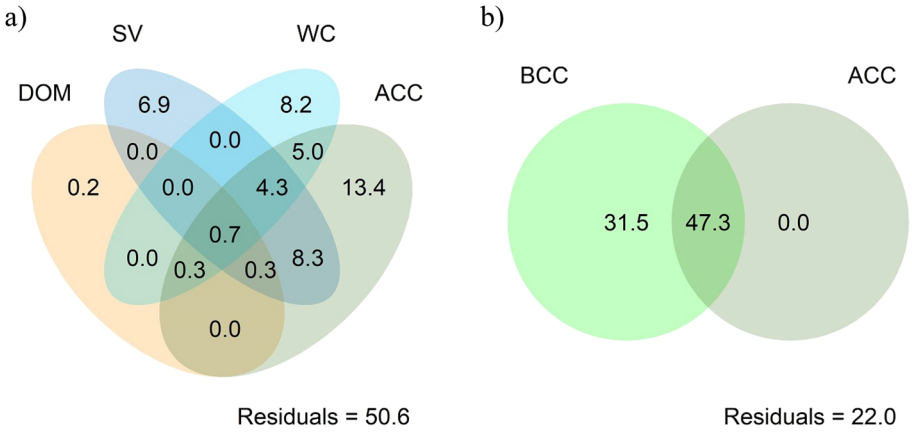

Fig. 4. (**a**) Variation partitioning of bacterial community composition (BCC) among algal community composition (ACC), water chemistry (WC), spatial variables (SV), and dissolved organic matter (DOM) ($n = 28$). (**b**) Variation partitioning of enzyme ratios among BCC and ACC ($n = 26$). The global redundancy analysis models with DOM and spatial variables as constraints were not significant and could thus not be used for the variation partitioning with enzyme ratios as response. Numbers represent percentage of variability explained.

11, spatial variable 13, and spatial variable 15 reflected small-scale variations across the river network.

The Vjosa River catchment is characterized by a highly diverse geology dominated by limestone, sandstone, flysch, and ultramafic igneous rock (Supporting Information Table S2). Geological variables explained 63% of the variation in water chemistry (i.e., Ca^{2+}, K^{+}, Mg^{2+}, S^{2-}, Si^{4+}, Na^{+}, SO_4^{2-}, Cl^{-}, NO_3^{-}, and conductivity) (redundancy analysis, global p-value <0.001; Supporting Information Fig. S1). Furthermore, from the water chemistry variables selected as important for the bacterial community, two out of five showed significant changes with increasing stream size (Supporting Information Fig. S4). Silica significantly decreased and sulfate significantly increased with increasing catchment area.

Absorbance- and spectrofluorometry-derived indices and dissolved organic carbon were used to describe DOM properties at each site and explain variation in bacterial community composition and enzyme ratios. $SUVA_{254}$, the only variable relevant for further analysis, is a proxy for aromaticity and was found to increase with increasing catchment area (Supporting Information Fig. S5). Dissolved organic carbon ranges between 0.23 and 4.45 mg L^{-1} and showed a tendency of decrease with increasing catchment area (Supporting Information Fig. S5).

Heterotrophic biofilm functioning is controlled by bacterial community composition

Variation partitioning of enzyme ratios showed that bacterial communities, more precisely bacterial principal components 1, 2, 6, and 8 explained 31.5% of the entire variation (Fig. 4b). In contrast to expectations of DOM to predict heterotrophic functioning, the global redundancy analysis model with DOM as predictor was not significant. The same is true for the global redundancy analysis model with spatial variables. The model with algal communities was significant and algal principal component 2 was selected. As expected, the algal community by itself did not explain any variation. However, bacterial and algal community compositions together accounted for 47.3% of the variation, leaving a total of 22% of the variation in enzyme ratios unexplained.

Correlating bacterial principal component 1 (gradient along DOM freshness and origin and small scale spatial patterns; *see* Supporting Information Fig. S6) and bacterial principal component 2 (gradient along catchment area, algal community, water chemistry, and aromaticity; *see* Supporting Information Fig. S6) with enzyme ratios underlined the strong linkage between the bacterial community and enzyme activities (Table 1). Bacterial principal component 1 showed significant correlations with all enzyme ratios, all of them other than Xyl/Glu correlated positively. Bacterial principal component 2 correlates negatively only to NAG/Pox and Cbh/Pox. We did not find any correlation between enzyme ratios and catchment area (Supporting Information Fig. S7).

Discussion

Metacommunity structure: Catchment area influences bacterial diversity and community composition

No other single environmental variable or trait of the terrestrial matrix correlated with bacterial diversity and community composition as strongly as catchment area (Fig. 2). The main pattern that we observed for bacterial community composition and diversity is a strong downstream homogenization, i.e., a significant decrease in variability with increasing stream size. This notion is consistent with findings from other studies (Besemer et al. 2013) and is thought to be the result of high environmental differentiation in headwaters leading to distinct community compositions (Besemer et al. 2013; Battin et al. 2016).

Table 1. Coefficient of determination (R^2) and significance (*p*-value) of Pearson's correlations between bacterial community composition principal components (BCC-PC), BCC-PC1 and BCC-PC2, and enzyme ratios ($n = 26$). Values in bold show significant correlations.

Enzyme ratios	BCC-PC1		BCC-PC2	
	R^2	*p*-value	R^2	*p*-value
Xyl/Glu	**−0.55**	**<0.01**	0.13	0.51
(Glu + Xyl)/Cbh	**0.60**	**<0.001**	−0.10	0.64
Glu/Pep	**0.63**	**<0.001**	0.13	0.53
Glu/NAG	**0.59**	**<0.01**	−0.05	0.8
NAG/Pox	**0.39**	**<0.05**	**−0.57**	**<0.01**
Cbh/Pox	**0.40**	**<0.05**	**−0.47**	**<0.05**
Glu/Pox	**0.44**	**<0.05**	−0.33	0.1

With downstream movement the potential colonizer pool increases and concomitantly environmental differentiation decreases leading to less variable benthic bacterial communities. Patterns in benthic bacterial community composition variability match between our findings and the results from Besemer et al. (2013). However, mean diversity showed opposing patterns with our results indicating an increase in diversity, albeit not significant (Fig. 2b), whereas Besemer et al. (2013) found a decrease in diversity with increasing stream size. Diversity of planktonic bacterial communities also showed contrasting patterns across stream size gradients, with studies finding both increased (Read et al. 2015) and decreased (Savio et al. 2015) diversity with increasing stream size. Hence, general assumptions for diversity patterns across stream size gradients prove difficult as bacterial habitats (e.g., benthic or planktonic), environmental variables, frequency of disturbances, or the scale of the network investigated can strongly differ between studies. Co-occurrence analysis revealed further changes in bacterial community composition across catchment area size classes. Both modularity and average path length decreased downstream (Fig. 3), indicating a decrease in available ecological niches (Faust and Raes 2012) and in resistance to perturbations (Faust and Raes 2012). These findings suggest that the further we move downstream, the more the bacterial community shifts from more clusters with strong interactions, to fewer bigger clusters. In other words, further downstream bacterial species occupy a more constraint available niche space. The observed increase in Chl *a* and decline in streamwater dissolved organic carbon with increasing catchment area (Supporting Information Figs. S2, S4) further support this notion. Chlorophyll *a* is a proxy for algal biomass and hence related to autochthonous DOM, while streamwater dissolved organic carbon is comprised of both, allochthonous and autochthonous material. Therefore, increasing algal biomass and decreasing streamwater dissolved organic carbon may enable more bacteria to co-exist with the same niche due to the higher availability of labile DOM. However, our study design was not aimed at testing these mechanisms and we therefore can only propose possible interpretations of these correlations.

Drivers of metacommunity structure: Bacterial community composition at river network scale is primarily driven by algae

Surprisingly, we found the algal community to explain the greatest share of the variation in the bacterial community (13.4%, Fig. 4a) suggesting that bacteria in biofilms undergo a strong species sorting process driven mainly by algae. Bacterial and algal communities both live in close proximity in benthic biofilms and exhibit strong bidirectional interactions. These interactions cover a variety of aspects such as provision of DOM and microhabitat structure through the algae and provision of micronutrients and macronutrients through the bacteria (Kouzuma and Watanabe 2015; Ramanan et al. 2016; Wagner et al. 2017). Likely, the most prominent mechanism through which algae affect bacteria in benthic biofilms is the production of autochthonous DOM, which can differ in quality depending on the algal communities and has been shown to affect bacteria (Bahulikar and Kroth 2008; Kouzuma and Watanabe 2015; Bengtsson et al. 2018). An additional explanation for the strong control of bacterial community composition by algae could be related to bacterial dispersal. The close proximity of algae and heterotrophic bacteria in benthic biofilms (Battin et al. 2016) may favor dispersal not only as single cells but also in the form of larger biofilm slabs (Costerton et al. 1995). Algae and bacteria form metacommunities (Leibold et al. 2004), which upon simultaneous dispersal may have similar spatial structure. Such non-independent co-dispersal of bacteria is known, for example, through attachment to zooplankton (Grossart et al. 2010). If the dispersal unit for bacteria (and algae) is a piece of detached biofilm (Boulêtreau et al. 2006), then species sorting pressure upon arrival at a suitable habitat may decrease substantially for bacteria, which are dependent on algae-derived resources. Taken together, these results create a new perspective on sorting vs. dispersal as drivers of benthic bacterial metacommunity structure. Metacommunity theory predicts that a local community is the result of "local" sorting of species from a "regionally" dispersing propagule pool. Our results suggest that resource-driven sorting of bacteria may not only occur locally in a growing benthic biofilm, but eventually even en route during dispersal of larger biofilm dispersal units that contain algae as the sorting agents themselves. Indeed, the river network-scale linkage of bacterial and algal communities can be viewed as a result of upstream sorting processes spreading downstream through biofilm dispersal units (Fig. 5).

More classical local species sorting processes may be tied to water chemistry (Lindström and Langenheder 2012). Indeed, the second largest portion of variation in bacterial community composition was explained by water chemistry with 8.2% (Fig. 4a). Recent findings suggest that species sorting is the

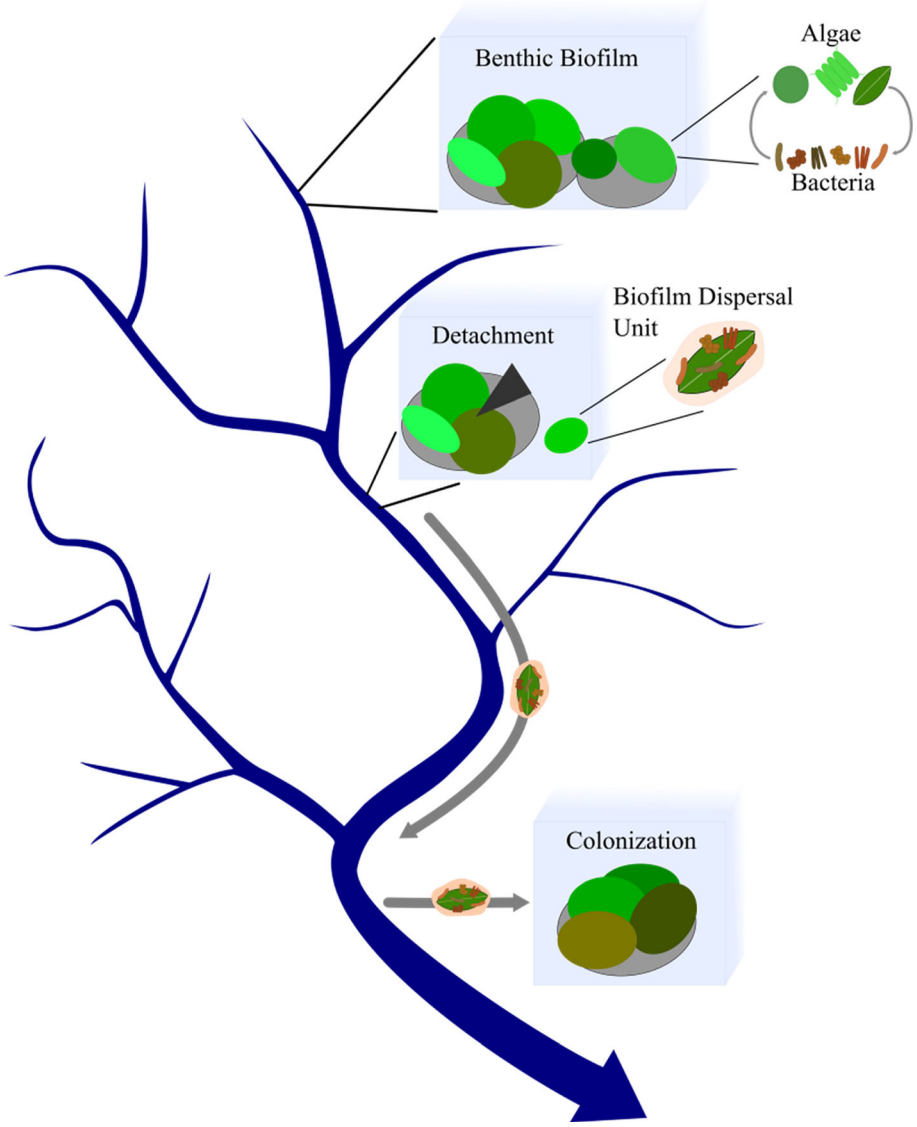

Fig. 5. Conceptual figure presenting simultaneous dispersal of algae and bacteria inhabiting benthic biofilms. In upstream regions, the interplay of isolation, mass effects, and species sorting drives community assembly of benthic biofilms. In suitable environmental conditions, well-adapted communities may emerge, characterized by close ties between algae and bacteria. Detachment of a piece of biofilm, for example, through hydraulic disturbance, enables co-dispersal and colonization of downstream habitats given suitable conditions. Contrary to single-cell dispersal, the advantage of this multicellular dispersal mode is an already well-established interaction between algae and bacteria reducing species sorting selection pressures upon arrival at a suitable habitat.

main driver of bacterial metacommunity assembly in freshwater ecosystems, explained by small size and rapid growth rates of bacteria (Van der Gucht et al. 2007; Heino et al. 2015). Our findings confirm that variables such as conductivity, which is closely related to geological features in the catchment, are among the most important local controls for bacterial community composition (Freimann et al. 2013). Water chemistry variables are strongly affected by our snapshot sampling design. However, good weather conditions during our field work make prominent temporal changes in local water chemistry (due to, e.g., heavy precipitation events) unlikely. Furthermore, the high geodiversity across the entire catchment describes a substantial fraction of variation in water chemistry (Supporting Information Fig. S1; 63% of variability in water chemistry explained by geo-principal components 1–4). Therefore, we are confident that our water chemistry data are representative for the respective local environmental conditions.

Spatial processes alone explained 6.9% of variation in benthic bacterial community composition (Fig. 4a). Variability in benthic bacterial communities explained by spatial variables indicates that in part the community is structured through dispersal limitations. Most variation was explained by spatial

variable 1, which strongly correlates with catchment area (Supporting Information Fig. S3). This comes as no surprise, as we found catchment area to be a strong predictor for both benthic bacterial community composition and diversity (Fig. 2).

Although previous work (Judd et al. 2006; Seballos et al. 2020) suggests that DOM composition and concentration are important drivers of bacterial community composition, we found that DOM variables alone explained very little of the variation in benthic bacteria (Fig. 4a). Dissolved organic matter variables in our study were strong indicators of terrigenous resource signatures and carried little imprint of autochthonous material. Algal exudates, which are considered highly labile (Murray et al. 1986; Romani and Sabater 2001), can vary depending on the algal community producing them and are mainly composed not only of carbohydrates, but also proteins and glycoproteins (Bahulikar and Kroth 2008; Wyatt et al. 2014; Fabian et al. 2018). In benthic biofilms, distinct algal communities can produce distinct combinations of algal exudates, shaping the bacteria therein (Bahulikar and Kroth 2008; Kalscheur et al. 2012). Our results show a limited linkage of bacterial community to terrigenous DOM (only $SUVA_{254}$ was retained as significant explanatory variable) and hence suggest a much higher importance of carbon sources within biofilms rather than from the catchment. In the context of DOM, the assumed strong linkage of bacterial and algal communities within biofilms (algae provide autochthonous, labile DOM to bacteria while bacteria provide inorganic carbon to algae) seems to support such strong internal carbon cycling (Battin et al. 2016; Ramanan et al. 2016). The relatively low dissolved organic carbon concentrations in the Vjosa River network (Supporting Information Fig. S5) may also force benthic bacteria to rely more on the autochthonous, algal-produced DOM. This does not rule out usage of terrigenous DOM from the water column by bacteria, but likely terrigenous signatures do not exert a strong selective pressure on the benthic bacterial communities.

Algal community composition structured by space and water chemistry also imprinted on the benthic bacterial communities with 8.3% and 5% of variability explained, respectively (Fig. 4a). This is not surprising as water chemistry and water turbidity, which both are strongly tied to geological conditions of the various subcatchments (Supporting Information Fig. S1), were identified as strong sorting agents for algae themselves (Fuß et al. 2024), and not just for bacteria. The same holds true for spatial processes (Fuß et al. 2024). On the other hand, this result also points to difficulties in separating a water chemistry-guided sorting process limited strictly to the local scale from a larger-scale water chemical imprint on benthic bacterial communities through co-dispersal with further upstream sorted algae in biofilm units. Indeed, water chemistry variables are tied to flowing water and will thus have a spatial structure more similar to those created by passive dispersal than any other environmental variable. A nearly equally large fraction of bacterial community composition was explained by algae, water chemistry, and spatial variables combined (4.3%). This highlights the importance of spatially structured water chemistry and the algal community (Fuß et al. 2024) which ultimately shape bacterial community composition.

Metacommunity structure–function coupling: Bacterial community composition drives heterotrophic biofilm functioning at the river network scale with little influence of large-scale resource patterns

The only significant single predictor for enzyme ratios was bacterial community composition, accounting for 31.5% of the variability, while DOM and spatial variables could not explain any variation (Fig. 4b). This suggests that throughout the Vjosa River network, different and distinct benthic bacterial communities are responsible for defined functional profiles, refuting the notion of functional redundancy at least for the measured enzymatic activities. Correlations of bacterial principal components 1 and 2 with most enzyme ratios support this notion (Table 1). Furthermore, the algal community was also selected as a significant covariate, but could not explain any variation by itself. As shared predictors bacterial and algal communities together accounted for 47.3% of variability (Fig. 4b). This result points once again to algae as strong sorting agents for the benthic bacterial communities suggesting direct control over bacterial community composition, which indirectly affects heterotrophic biofilm functioning. This notion further underlines the strong link between bacterial and algal communities at the microhabitat scale. A possible mechanism through which these strong associations affect heterotrophic functioning is the reduced mismatch between bacterial and resource traits as already shown for benthic communities (Kalscheur et al. 2012; Battin et al. 2016; Fabian et al. 2018). The fact that sorting-driven turnover of community composition drives functioning more than neutrally driven turnover (associated with limited or very intense dispersal), was also a major outcome of a comparative study on algae in the same river network (Fuß et al. 2024). Conceptually, we propose that benthic bacterial biofilm functioning varies along (micro-)habitat gradients, which are largely driven by traits of distinct bacterial communities and their strong interaction with algae co-occurring in the same biofilm. Our study design does not allow to directly unravel the mechanisms behind algal–bacterial interactions, yet the results suggest that production of algal exudates and the provision of microhabitat structure directly sort the benthic bacterial community and hence distally control the resulting bacterial functioning.

Conclusion

Turnover phenomena in community composition of benthic bacteria and algae have mostly been researched as standalone compartments within riverine biofilms. Here we present evidence that benthic bacterial communities are mainly controlled by the composition of co-occurring algae living in close proximity, suggesting a strong bacterial–algal

link in benthic biofilms across the whole river network. This result and the consideration of co-dispersal of bacteria and algae in biofilm dispersal units highlight the need for more holistic research approaches to understand spatial–temporal dynamics and hence the ecology of in-stream biofilm communities. Multitrophic biofilm metacommunities may indeed be better understood when modeled under explicit consideration of biotic interactions (Kouzuma and Watanabe 2015; Ramanan et al. 2016; Leibold et al. 2020). Spatial processes exert additional control on the bacterial community composition, highlighting the downstream homogenization found for riverine benthic bacterial communities and diversity. In turn, the spatially structured bacterial community was the strongest predictor of enzyme ratios across the entire network underscoring the strong linkage between bacterial community composition and the resulting heterotrophic biofilm functioning. Furthermore, the strong control of algae on the bacterial communities was evident when looking at enzyme ratios, as most of the variation was explained by bacterial and algal communities together. This suggests that the benthic biofilm in a well-preserved river as the Vjosa is structurally and functionally shaped by the strong algal–bacterial link through a presumably strong coupling between algal exudates and bacterial heterotrophic functioning. Maintaining this link may be related to the preservation of the near-natural and hydromorphological intact Vjosa River network, which recently has been given protected status as Europe's first Wild River National Park. To ensure real ecosystem conservation, it may be key to maintain structure and function of the network-wide biofilm community.

Data availability statement

Datasets used in this study are available at Figshare under DOI 10.6084/m9.figshare.25837993.v2 and the CC BY 4.0 license.

References

Bahulikar, R. A., and P. G. Kroth. 2008. The complex extracellular polysaccharides of mainly chain-forming freshwater diatom species from epilithic biofilms. J. Phycol. **44**: 1465–1475. doi:10.1111/j.1529-8817.2008.00609.x

Battin, T. J., L. A. Kaplan, J. Newbold, and C. Hansen. 2003. Contributions of microbial biofilms to ecosystem processes in stream mesocosms. Nature **426**: 439–442.

Battin, T. J., K. Besemer, M. M. Bengtsson, A. M. Romani, and A. I. Packmann. 2016. The ecology and biogeochemistry of stream biofilms. Nat. Rev. Microbiol. **14**: 251–263. doi:10.1038/nrmicro.2016.15

Benda, L., N. L. Poff, D. Miller, T. Dunne, G. Reeves, G. Pess, and M. Pollock. 2004. The network dynamics hypothesis: How channel networks structure riverine habitats. Bioscience **54**: 413. doi:10.1641/0006-3568(2004)054[0413:TNDHHC]2.0.CO;2

Bengtsson, M. M., K. Wagner, C. Schwab, T. Urich, and T. J. Battin. 2018. Light availability impacts structure and function of phototrophic stream biofilms across domains and trophic levels. Mol. Ecol. **27**: 2913–2925. doi:10.1111/mec.14696

Besemer, K., G. Singer, C. Quince, E. Bertuzzo, W. Sloan, and T. J. Battin. 2013. Headwaters are critical reservoirs of microbial diversity for fluvial networks. Proc. R. Soc. B Biol. Sci. **280**: 20131760. doi:10.1098/rspb.2013.1760

Blanchet, F. G., P. Legendre, and D. Borcard. 2008*a*. Modelling directional spatial processes in ecological data. Ecol. Model. **215**: 325–336. doi:10.1016/j.ecolmodel.2008.04.001

Blanchet, F. G., P. Legendre, and D. Borcard. 2008*b*. Forward selection of explanatory variables. Ecology **89**: 2623–2632. doi:10.1890/07-0986.1

Blanchet, F. G., P. Legendre, R. Maranger, D. Monti, and P. Pepin. 2011. Modelling the effect of directional spatial ecological processes at different scales. Oecologia **166**: 357–368. doi:10.1007/s00442-010-1867-y

Blanchet, F. G., P. Legendre, J. A. C. Bergeron, and F. He. 2014. Consensus RDA across dissimilarity coefficients for canonical ordination of community composition data. Ecological monographs **84**: 491–511. doi:10.1890/13-0648.1

Blanchet, F. G., P. Legendre, and O. Gauthier. 2015. AEM: Tools to construct asymmetric eigenvector maps (AEM) spatial variables. R package version 0.6/r127. Available from https://R-Forge.R-project.org/projects/sedar/

Boulêtreau, S., F. Garabétian, S. Sauvage, and J. M. Sánchez-Pérez. 2006. Assessing the importance of a self-generated detachment process in river biofilm models. Freshw. Biol. **51**: 901–912. doi:10.1111/j.1365-2427.2006.01541.x

Callahan, B. J., P. J. McMurdie, M. J. Rosen, A. W. Han, A. J. A. Johnson, and S. P. Holmes. 2016. DADA2: High-resolution sample inference from Illumina amplicon data. Nat. Methods **13**: 581–583. doi:10.1038/nmeth.3869

Cardinale, B. J., M. A. Palmer, and S. L. Collins. 2002. Species diversity enhances ecosystem functioning through interspecific facilitation. Nature **415**: 426–429. doi:10.1038/415426a

Clauset, A., M. E. J. Newman, and C. Moore. 2004. Finding community structure in very large networks. Phys. Rev. E **70**: 066111. doi:10.1103/PhysRevE.70.066111

Costerton, J. W., Z. Lewandowski, D. E. Caldwell, D. R. Korber, and H. M. Lappin-Scott. 1995. Microbial biofilms. Annu. Rev. Microbiol. **19**: 711–745.

Creed, I. F., and others. 2015. The river as a chemostat: Fresh perspectives on dissolved organic matter flowing down the river continuum. Can. J. Fish. Aquat. Sci. **72**: 1272–1285. doi:10.1139/cjfas-2014-0400

Crump, B. C., L. A. Amaral-Zettler, and G. W. Kling. 2012. Microbial diversity in arctic freshwaters is structured by inoculation of microbes from soils. ISME J. **6**: 1629–1639. doi:10.1038/ismej.2012.9

Csardi, G., and T. Nepusz. 2006. The igraph software package for complex network research. J. Complex Syst. **1695**: 2191–2193. doi:10.3724/sp.j.1087.2009.02191

Delgado-Baquerizo, M., L. Giaramida, P. B. Reich, A. N. Khachane, K. Hamonts, C. Edwards, L. A. Lawton, and B. K. Singh. 2016. Lack of functional redundancy in the relationship between microbial diversity and ecosystem functioning. J. Ecol. **104**: 936–946. doi:10.1111/1365-2745.12585

Dray, S., P. Legendre, and P. R. Peres-Neto. 2006. Spatial modelling: A comprehensive framework for principal coordinate analysis of neighbour matrices (PCNM). Ecol. Model. **196**: 483–493. doi:10.1016/j.ecolmodel.2006.02.015

Dray, S., P. Legendre, and G. Blanchet. 2016. packfor: Forward Selection with permutation (Canoco). p. 46.

European Geological Data Infrastructure. 2018. EGDI 1:1 million pan-European surface geology. http://www.europe-geology.eu

Fabian, J., S. Zlatanović, M. Mutz, H.-P. Grossart, R. van Geldern, A. Ulrich, G. Gleixner, and K. Premke. 2018. Environmental control on microbial turnover of leaf carbon in streams—Ecological function of phototrophic-heterotrophic interactions. Front. Microbiol. **9**: 1–16. doi:10.3389/fmicb.2018.01044

Faust, K., and J. Raes. 2012. Microbial interactions: From networks to models. Nat. Rev. Microbiol. **10**: 538–550. doi:10.1038/nrmicro2832

Fell, S. C., and others. 2021. Fungal decomposition of river organic matter accelerated by decreasing glacier cover. Nat. Clim. Chang. **11**: 349–353. doi:10.1038/s41558-021-01004-x

Findlay, S., and R. L. Sinsabaugh. 2006. Large-scale variation in subsurface stream biofilms: A cross-regional comparison of metabolic function and community similarity. Microb. Ecol. **52**: 491–500. doi:10.1007/s00248-006-9095-z

Freimann, R., H. Bürgmann, S. E. G. Findlay, and C. T. Robinson. 2013. Bacterial structures and ecosystem functions in glaciated floodplains: Contemporary states and potential future shifts. ISME J. **7**: 2361–2373. doi:10.1038/ismej.2013.114

Freixa, A., E. Ejarque, S. Crognale, S. Amalfitano, S. Fazi, A. Butturini, and A. M. Romaní. 2016. Sediment microbial communities rely on different dissolved organic matter sources along a Mediterranean river continuum. Limnol. Oceanogr. **61**: 1389–1405. doi:10.1002/lno.10308

Friedman, J., and E. J. Alm. 2012. Inferring correlation networks from genomic survey data. PLoS Comput. Biol. **8**: e1002687. doi:10.1371/journal.pcbi.1002687

Fuß, T., B. Behounek, A. J. Ulseth, and G. A. Singer. 2017. Land use controls stream ecosystem metabolism by shifting dissolved organic matter and nutrient regimes. Freshw. Biol. **62**: 582–599. doi:10.1111/fwb.12887

Fuß, T., L. Thuile Bistarelli, F. Walther, S. Vitecek, L. Talluto, and G. Singer. 2024. Geodiversity of a European river network controls algal biodiversity and function. Commun. Earth Environ. **5**: 315. doi:10.1038/s43247-024-01478-5

Grossart, H.-P., C. Dziallas, F. Leunert, and K. W. Tang. 2010. Bacteria dispersal by hitchhiking on zooplankton. Proc. Natl. Acad. Sci. USA **107**: 11959–11964. doi:10.1073/pnas.1000668107

Gweon, H. S., M. J. Bowes, H. L. Moorhouse, A. E. Oliver, M. J. Bailey, M. C. Acreman, and D. S. Read. 2021. Contrasting community assembly processes structure lotic bacteria metacommunities along the river continuum. Environ. Microbiol. **23**: 484–498. doi:10.1111/1462-2920.15337

Heino, J., A. S. Melo, T. Siqueira, J. Soininen, S. Valanko, and L. M. Bini. 2015. Metacommunity organisation, spatial extent and dispersal in aquatic systems: Patterns, processes and prospects. Freshw. Biol. **60**: 845–869. doi:10.1111/fwb.12533

Helms, J. R., A. Stubbins, J. D. Ritchie, E. C. Minor, D. J. Kieber, and K. Mopper. 2008. Absorption spectral slopes and slope ratios as indicators of molecular weight, source, and photobleaching of chromophoric dissolved organic matter. Limnol. Oceanogr. **53**: 955–969. doi:10.4319/lo.2008.53.3.0955

Institute of Geological Research and the Oil and Gas Institute of Albania. 2002. Harta gjeologjike e shqiperise (geological map of Albania). 1:200 000.

Judd, K. E., B. C. Crump, and G. W. Kling. 2006. Variation in dissolved organic matter controls bacterial production and community composition. Ecology **87**: 2068–2079. doi:10.1890/0012-9658(2006)87[2068:vidomc]2.0.co;2

Kalscheur, K. N., M. Rojas, C. G. Peterson, J. J. Kelly, and K. A. Gray. 2012. Algal exudates and stream organic matter influence the structure and function of denitrifying bacterial communities. Microb. Ecol. **64**: 881–892. doi:10.1007/s00248-012-0091-1

Klindworth, A., E. Pruesse, T. Schweer, J. Peplies, C. Quast, M. Horn, and F. O. Glöckner. 2013. Evaluation of general 16S ribosomal RNA gene PCR primers for classical and next-generation sequencing-based diversity studies. Nucleic Acids Res. **41**: e1. doi:10.1093/nar/gks808

Kouzuma, A., and K. Watanabe. 2015. Exploring the potential of algae/bacteria interactions. Curr. Opin. Biotechnol. **33**: 125–129. doi:10.1016/j.copbio.2015.02.007

Kurtz, Z. D., C. L. Müller, E. R. Miraldi, D. R. Littman, M. J. Blaser, and R. A. Bonneau. 2015. Sparse and compositionally robust inference of microbial ecological networks C. PLoS Comput. Biol. **11**: e1004226. doi:10.1371/journal.pcbi.1004226

Leibold, M. A., and others. 2004. The metacommunity concept: A framework for multi-scale community ecology. Ecol. Lett. **7**: 601–613. doi:10.1111/j.1461-0248.2004.00608.x

Leibold, M. A., and others. 2020. The internal structure of metacommunities. *bioRxiv*.

Lindström, E. S., and S. Langenheder. 2012. Local and regional factors influencing bacterial community assembly. Environ. Microbiol. Rep. **4**: 1–9. doi:10.1111/j.1758-2229.2011.00257.x

Loreau, M., S. Naeem, and P. Inchausti. 2001. Biodiversity and ecosystem functioning: Current knowledge and future challenges. Science **294**: 804–808.

Loreau, M., N. Mouquet, and R. D. Holt. 2003. Meta-ecosystems: A theoretical framework for a spatial

ecosystem ecology. Ecol. Lett. **6**: 673–679. doi:10.1046/j.1461-0248.2003.00483.x

Louca, S., and others. 2018. Function and functional redundancy in microbial systems. Nat. Ecol. Evol. **2**: 936–943. doi:10.1038/s41559-018-0519-1

McKnight, D. M., E. W. Boyer, P. K. Westerhoff, P. T. Doran, T. Kulbe, and D. T. Andersen. 2001. Spectrofluorometric characterization of dissolved organic matter for indication of precursor organic material and aromaticity. Limnol. Oceanogr. **46**: 38–48. doi:10.4319/lo.2001.46.1.0038

Mosher, J. J., L. a. Kaplan, D. C. Podgorski, A. M. McKenna, and A. G. Marshall. 2015. Longitudinal shifts in dissolved organic matter chemogeography and chemodiversity within headwater streams: A river continuum reprise. Biogeochemistry **124**: 371–385. doi:10.1007/s10533-015-0103-6

Murray, R. E., K. E. Cooksey, and J. C. Priscu. 1986. Stimulation of bacterial DNA synthesis by algal exudates in attached algal–bacterial consortia. Appl. Environ. Microbiol. **52**: 1177–1182. doi:10.1128/AEM.52.5.1177-1182.1986

Nercessian, O., E. Noyes, M. G. Kalyuzhnaya, M. E. Lidstrom, and L. Chistoserdova. 2005. Bacterial populations active in metabolism of C1 compounds in the sediment of lake Washington, a freshwater lake. Appl. Environ. Microbiol. **71**: 6885–6899.

Niederdorfer, R., H. Peter, and T. J. Battin. 2016. Attached biofilms and suspended aggregates are distinct microbial lifestyles emanating from differing hydraulics. Nat. Microbiol. **1**: 16178. doi:10.1038/nmicrobiol.2016.178

Oksanen, J., and others. 2019. vegan: Community Ecology Package.

Pérez, M. T., and R. Sommaruga. 2006. Differential effect of algal- and soil-derived dissolved organic matter on alpine lake bacterial community composition and activity. Limnol. Oceanogr. **51**: 2527–2537. doi:10.4319/lo.2006.51.6.2527

Quantum GIS Development Team. 2015. Quantum GIS geographic information system. Open Source Geospatial Found. Proj. http://qgis.osgeo.org

R Development Core Team. 2014. R: A language and environment for statistical computing. http://www.r-project.org

Ramanan, R., B.-H. Kim, D.-H. Cho, H.-M. Oh, and H.-S. Kim. 2016. Algae–bacteria interactions: Evolution, ecology and emerging applications. Biotechnol. Adv. **34**: 14–29. doi:10.1016/j.biotechadv.2015.12.003

Raymond, P. A., J. E. Saiers, and W. V. Sobczak. 2016. Hydrological and biogeochemical controls on watershed dissolved organic matter transport: Pulse-shunt concept. Ecology **97**: 5–16. doi:10.1890/14-1684.1

Read, D. S., H. S. Gweon, M. J. Bowes, L. K. Newbold, D. Field, M. J. Bailey, and R. I. Griffiths. 2015. Catchment-scale biogeography of riverine bacterioplankton. ISME J. **9**: 516–526. doi:10.1038/ismej.2014.166

Rigby, R. A., and D. M. Stasinopoulos. 2005. Generalized additive models for location, scale and shape (with discussion). J. R. Stat. Soc. Ser. C Appl, Stat. **54**: 507–554. doi:10.1111/j.1467-9876.2005.00510.x

Romani, A. M., and S. Sabater. 2001. Structure and activity of rock and sand biofilms in a Mediterranean stream. Ecology **82**: 3232–3245. doi:10.1890/0012-9658(2001)082[3232:SAAORA]2.0.CO;2

Romaní, A. M., H. Guasch, I. Munoz, J. Ruana, E. Vilalta, T. Schwartz, F. Emtiazi, and S. Sabater. 2004. Biofilm structure and function and possible implications for riverine DOC dynamics. Microb. Ecol. **47**: 316–328. doi:10.1007/s00248-003-2019-2

Romaní, A. M., J. Artigas, and I. Ylla. 2012. Extracellular enzymes in aquatic biofilms: Microbial interactions versus water quality effects in the use of organic matter, p. 153–174. *In* Microbial biofilms: Current research and applications. Caister Academic.

Savio, D., and others. 2015. Bacterial diversity along a 2600 km river continuum. Environ. Microbiol. **17**: 4994–5007. doi:10.1111/1462-2920.12886

Schiemer, F., and others. 2020. The Vjosa River corridor: A model of natural hydro-morphodynamics and a hotspot of highly threatened ecosystems of European significance. Landsc. Ecol. **35**: 953–968. doi:10.1007/s10980-020-00993-y

Seballos, R., K. Wyatt, R. Bernot, S. Brown, S. Chandra, and A. Rober. 2020. Nutrient availability and organic matter quality shape bacterial community structure in a lake biofilm. Aquat. Microb. Ecol. **85**: 1–18. doi:10.3354/ame01937

Singer, G., K. Besemer, G. Hochedlinger, A. Chlup, and T. Battin. 2011. Monomeric carbohydrate uptake and structure–function coupling in stream biofilms. Aquat. Microb. Ecol. **62**: 71–83. doi:10.3354/ame01454

Talluto, M. 2019. WatershedTools: Tools for watershed analysis. R package version 1.0.1.9013.

Talluto, M., R. del Campo, E. Estévez, F. Altermatt, T. Datry, and G. Singer. 2024. Towards (better) fluvial metaecosystem ecology: A research perspective. npj Biodivers. **3**: 3. doi:10.1038/s44185-023-00036-0

Van der Gucht, K., and others. 2007. The power of species sorting: Local factors drive bacterial community composition over a wide range of spatial scales. Proc. Natl. Acad. Sci. U.S.A. **104**: 20404–20409. doi:10.1073/pnas.0707200104

Wagner, K., M. M. Bengtsson, R. H. Findlay, T. J. Battin, and A. J. Ulseth. 2017. High light intensity mediates a shift from allochthonous to autochthonous carbon use in phototrophic stream biofilms. J. Geophys. Res. Biogeosci. **122**: 1806–1820. doi:10.1002/2016JG003727

Weishaar, J. L., G. R. Aiken, B. A. Bergamaschi, M. S. Fram, R. Fujii, and K. Mopper. 2003. Evaluation of specific ultraviolet absorbance as an indicator of the chemical composition and reactivity of dissolved organic carbon. Environ. Sci. Technol. **37**: 4702–4708. doi:10.1021/es030360x

Wisnoski, N. I., and J. T. Lennon. 2021. Microbial community assembly in a multi-layer dendritic metacommunity. Oecologia **195**: 13–24. doi:10.1007/s00442-020-04767-w

Wyatt, K. H., A. R. Rober, N. Schmidt, and I. R. Davison. 2014. Effects of desiccation and rewetting on the release and decomposition of dissolved organic carbon from benthic macroalgae. Freshw. Biol. **59**: 407–416. doi:10.1111/fwb.12273

Zancarini, A., I. Echenique-Subiabre, D. Debroas, N. Taïb, C. Quiblier, and J.-F. Humbert. 2017. Deciphering biodiversity and interactions between bacteria and microeukaryotes within epilithic biofilms from the Loue River, France. Sci. Rep. **7**: 4344. doi:10.1038/s41598-017-04016-w

Zsolnay, A., E. Baigar, M. Jimenez, B. Steinweg, and F. Saccomandi. 1999. Differentiating with fluorescence spectroscopy the sources of dissolved organic matter in soils subjected to drying. Chemosphere **38**: 45–50. doi:10.1016/S0045-6535(98)00166-0

Acknowledgments

We thank Sajmir Beqiraj, Emil Birnstiel, Sonia Herrero Ortega, Barbara Stein, Remo Wüthrich, and the water chemical laboratory at IGB Berlin for support in the field and in the lab. Financial support came from the project FLUFLUX (ERC-2016-STG 716196).

Conflict of Interest

None declared.

Submitted 30 May 2024
Revised 27 August 2024
Accepted 01 September 2024

Associate Editor: Michaela Salcher